

The N- and C-terminal autolytic fragments of CAPN3/p94/calpain-3 restore proteolytic activity by intermolecular complementation

Yasuko Ono^{a,b,1}, Mayumi Shindo^c, Naoko Doi^a, Fujiko Kitamura^a, Carol C. Gregorio^b, and Hiroyuki Sorimachi^a

^aDepartment of Advanced Science for Biomolecules, Calpain Project, and ^cAdvanced Technical Support Department, Basic Technology Research Center, Tokyo Metropolitan Institute of Medical Science (IGAKUKEN), Setagaya-ku, Tokyo 156-8506, Japan; and ^bCellular and Molecular Medicine and Sarver Molecular Cardiovascular Research Program, University of Arizona, Tucson, AZ 85724

Edited by Vishva M. Dixit, Genentech, San Francisco, CA, and approved November 5, 2014 (received for review June 26, 2014)

CAPN3/p94/calpain-3, a calpain protease family member predominantly expressed in skeletal muscle, possesses unusually rapid and exhaustive autolytic activity. Mutations in the human CAPN3 gene impairing its protease functions cause limb-girdle muscular dystrophy type 2A (LGMD2A); yet, the connection between CAPN3's autolytic activity and the enzyme's function in vivo remain unclear. Here, we demonstrated that CAPN3 protease activity was reconstituted by intermolecular complementation (iMOC) between its two autolytic fragments. Furthermore, the activity of full-length CAPN3 active-site mutants was surprisingly rescued through iMOC with autolytic fragments containing WT amino acid sequences. These results provide evidence that WT CAPN3 can be formed by the iMOC of two different complementary CAPN3 mutants. The finding of iMOC-mediated restoration of calpain activity indicates a novel mechanism for the genotype–phenotype links in LGMD2A.

calpain | skeletal muscle | muscular dystrophy | complementation | protease

CAPN3 (also known as p94 or calpain-3) belongs to the calpain super family (EC3.4.22.18, clan CA, family C2) (1, 2). The consensus protease core sequence referred to as “CysPc” (cd00044 in the conserved domain database of the National Center for Biotechnology Information, NCBI) is shared by gene products belonging to the calpain super family. Because CAPN3 has calpain-type beta-sandwich (CBSW) and penta-EF-hand [PEF(L)] domains, it is classified as a “classical” calpain (3–5). Structural studies have revealed that calpain's Ca²⁺-requiring protease activity is mediated by Ca²⁺ binding to the CysPc domain (6–10). This property has been difficult to capture biochemically for some calpains using conventional assay methods.

CAPN3 undergoes an apparently Ca²⁺-independent and exhaustive autolysis in several ex vivo protein-expressing systems, which has marked this calpain species as an intriguing yet intractable subject in the research field (11). CAPN3, on the other hand, can be stably expressed in skeletal muscle cells where endogenous CAPN3 is predominantly found (12). The autolytic activity of CAPN3 is dependent upon the presence of the CAPN3-specific insertion sequences, IS1 and IS2 (Fig. 1A) (11). The mechanism(s) by which these insertions transform CAPN3, which is otherwise quite similar to those of CAPN1 and CAPN2 with the exception of the interactions with the calpain small subunit (CAPNS1), into being highly autolytic, is not yet clear. Although it is known that CAPN3 avoids “random” autolysis in skeletal muscle by associating with specific binding proteins such as titin and PLEIAD/SIMC1, the general regulation of CAPN3 autolysis in vivo is still poorly understood (13–16).

After CAPN3 was identified as the gene responsible for limb-girdle muscular dystrophy type 2A (LGMD2A), various aspects of CAPN3's biological function were intensively studied (17). Studies using transgenic knockout (KO) (18–23), as well as knockin (KI) mice (24, 25) demonstrated that defective CAPN3 protease activity is the primary cause for the disease. In vitro analyses of the CAPN3

missense mutations found in patients with LGMD2A suggested that both the loss of apparent Ca²⁺-independent autolyzing activity and, in contrast, the excess expression of autolyzing activity are associated with the improper function of the CAPN3 mutants (26). The biological significance of the peculiar autolytic activity associated with CAPN3 is yet to be defined.

It was reported that autolysis of CAPN3 in the IS1 region alters the accessibility of substrates as well as inhibitors to its protease core, indicating that autolysis is positively involved in the activation of CAPN3 (27). In addition, studies, including ours, suggested that the autolyzed fragments of CAPN3 remain associated as an active protease (27–29). Such an interaction was, however, considered temporary. Also, there is a notion that down-regulation of CAPN3 is an important outcome of autolysis based on the fact that the overexpression of wild-type (WT) CAPN3 in mouse skeletal muscle was not found to be harmful, whereas the overexpression of CAPN3:ΔIS1, whose autolytic but not proteolytic activity is attenuated (30), causes the development of a degenerating skeletal muscle phenotype (31). Thus, CAPN3's extremely strong propensity to autolyze may contribute to the regulation of its protease activity in both positive and negative directions.

Possible interactions between two CAPN3 molecules have also been investigated. Studies focusing on homodimerization of CAPN3 have revealed the unique feature in the C-terminal PEF(L) domain (32, 33). With respect to the pathological mechanisms of

Significance

CAPN3/p94/calpain-3, a calpain protease family member, has uniquely rapid and exhaustive autolytic activity. Here, we demonstrate that active protease core domain of CAPN3 is reconstituted by de novo intermolecular complementation (iMOC) between its two autolytic fragments. We also show that iMOC between one of the autolytic fragments and an unautolyzed full-length CAPN3 effectively generates autolytic activity. So far, CAPN3 is the only example of calpain that exhibits activity mediated by intermolecular complementation of its autolytic products. Mutations in the human CAPN3 gene cause limb-girdle muscular dystrophy type 2A (LGMD2A or calpainopathy). Understanding the genotype–phenotype links in the pathology of LGMD2A will be accelerated by incorporating iMOC-CAPN3 as one of active CAPN3 entities.

Author contributions: Y.O. designed research; Y.O., M.S., N.D., and F.K. performed research; M.S. contributed new reagents/analytic tools; Y.O., M.S., C.C.G., and H.S. analyzed data; and Y.O., C.C.G., and H.S. wrote the paper.

The authors declare no conflict of interest.

This article is a PNAS Direct Submission.

Freely available online through the PNAS open access option.

¹To whom correspondence should be addressed. Email: ono-ys@igakuken.or.jp.

This article contains supporting information online at www.pnas.org/lookup/suppl/doi:10.1073/pnas.1411959111/-DCSupplemental.

Results

CAPN3 Autolytic Fragments Reconstitute an Active Protease Complex Through iMOC.

As an early event of autolysis, CAPN3 is proteolyzed within or close to the IS1 region, generating N- and C-terminal fragments containing the active-site amino acid residues (aars), Cys129, and His334 and Asn358, respectively (Fig. 1A, N_{31K} and C_{58K}). “N_{xxK}” represents an N-terminal fragment containing PC1 and part of PC2, exhibiting a relative molecular mass (M_r) of xx kDa (“Nterm” inclusively refers to these fragments). “C_{xxK}” represents a C-terminal fragment encompassing part of PC2 and the rest of the C-terminal domain, exhibiting a M_r of xx kDa (“Cterm” inclusively refers to these fragments). To explore the possibility that two different CAPN3 mutants compensate for each other and reconstitute the active enzyme following autolysis, two nonoverlapping autolytic fragments of CAPN3 represented as the constructs N_{31K} (amino acid region 1–274) and C_{58K} (amino acid region 323–821) (Fig. 1A) were coexpressed to determine whether they had the propensity to generate protease activity similar to that of intact CAPN3. To detect proteolytic activity, C-terminal binding protein 1 (CTBP1), which functions as a substrate for CAPN3 (16) was used (Fig. 2A).

When MYC-epitope tagged-CTBP1 (Fig. 2A, Upper Scheme) was coexpressed with CAPN3:WT in COS7 cells, a MYC-labeled proteolytic fragment was generated (Fig. 2B, lane 2, anti-MYC) (16). Similarly, the coexpression of N_{31K} and C_{58K} also resulted in the proteolysis of MYC-CTBP1 (Fig. 2B, lane 3). However, when the two catalytic amino acid residues in C_{58K}, His and Asn, were replaced by Ala, CTBP1’s proteolysis was suppressed (Fig. 2B, lane 4). These results showed that proteolytic activity was generated through cooperation of the catalytic amino acid residues residing in two independently synthesized protein fragments, and suggest that autolytic fragments from different CAPN3 molecules can reconstitute protease activity through iMOC. Further autolysis by reconstituted CAPN3 activity was also observed (Fig. 2B, anti-C3IS2, lane 3).

The N-Terminal Region of CAPN2 Can Undergo iMOC with the C-Terminal Autolyzed Fragment of CAPN3.

To determine whether the observed iMOC is CAPN3 specific, the CAPN2:N_{27K} fragment was used in place of CAPN3 N_{31K}. CAPN2:N_{27K} corresponds to CAPN3 N_{30K}, which is 7 aars shorter than N_{31K} and lacks the IS1 sequence (Fig. 1A). Surprisingly, CAPN2:N_{27K} was able to substitute for N_{31K}, resulting in CTBP1 proteolysis (Fig. 2C, lane 4 vs. lanes 2 and 3). We further verified that the reconstituted proteolytic activity was dependent on the active-site Cys105 residue of CAPN2 (lane 5) as well as that CAPN2:N_{27K} interacted with C_{58K} (Fig. S1A). Because CAPN2 lacks CAPN3-specific N-terminal insertion sequence (NS), this result indicates that both NS and IS1 in CAPN3 are dispensable for the iMOC mediated by autolytic fragments, and that the N-terminal domains from different calpain species can undergo iMOC.

The Specificity of CAPN3 iMOC Resides in Its C-Terminal Autolytic Fragment but Does Not Require IS2.

When N_{30K} was coexpressed with C_{58K}: Δ IS2 together with MYC-CTBP1 in COS7 cells, CTBP1 proteolysis was observed (Fig. 2D, anti-MYC; lane 5 vs. lanes 3 and 4). Therefore, in addition to IS1, IS2 was also dispensable for the iMOC-mediated protease activity of CAPN3. On the other hand, CAPN2:C_{53K}, which corresponds to CAPN3 C_{58K}: Δ IS2, did not undergo detectable iMOC with N_{30K}, as evaluated by CTBP1 proteolysis (Fig. 2D, lanes 6 and 7). These results indicate that the iMOC-mediated protease activity of CAPN3 was dependent on sequences in its C-terminal region, but that IS2 was not required. Although the C-terminal region corresponding to CAPN3 C_{58K} is less conserved than the N-terminal region, it is still highly similar to the corresponding regions in CAPN1 and -2 (Fig. S2B). We could not identify any specific C-terminal sequences that were unique to CAPN3, indicating that the C-terminal specificity

that contributes to CAPN3-mediated iMOC may be attributed to the secondary structure of this region.

β -Strand Structures in PC2 Contribute to the Formation of iMOC-CAPN3.

To gain further insight into the molecular mechanism of iMOC, we referred to the structure of the Ca²⁺-bound form of rat CAPN2/CAPNS1. In PC2, an antiparallel β -sheet was formed by the insertion of β -strand 6 (β_6) between β_1 and β_2 (Figs. S2 and S3) (6). In a previous study, it was suggested that the corresponding structure in PC2 of CAPN3 supports the association of autolytic fragments after autolysis in IS1 (27). Thus, we examined the contribution of the β -strands in PC2 to iMOC-mediated CAPN3 protease activity using N_{29K}, which lacks these structures (Fig. 1A and Fig. S3). Because N_{29K} coexpressed with C_{58K} did not reconstitute CTBP1 proteolysis (Fig. 2E, lane 3) or coimmunoprecipitate with C_{58K} (Fig. S1B), we concluded that the β_2 strands in the PC2 domain of CAPN3 were required for the interaction of the autolyzed fragments.

iMOC-Generated CAPN3 Exhibits Substantial Autolysis.

To compare cellular targets of WT and iMOC-mediated CAPN3 protease activity, proteomic differences in COS7 cells expressing either form of CAPN3 were analyzed using reagents for isobaric tagging to determine the relative and absolute amounts quantitatively (iTRAQ). This experiment is anticipated to find possible substrates differentially proteolyzed by two forms of CAPN3. As a protease-inactive control for FL-CAPN3, FL:SHN has been sufficient; however, for the iMOC-CAPN3, all three catalytic amino acids were replaced with Ala to minimize nonspecific activity.

Under both conditions, among the proteins identified with more than five peptides, CAPN3 itself and coexpressed CTBP1 were significantly down-regulated (Fig. 3). In contrast, calpastatin (CAST), a previously established substrate for CAPN3, was efficiently more down-regulated only in cells expressing FL-CAPN3 (1.61 vs. 1.14). In COS7 cells, however, it was suggested that complementation generates activity at an efficiency of less than 5% of FL-CAPN3 activation (Fig. S4). Therefore, the possibility that CAST is a differential substrate candidate for FL- and iMOC-CAPN3, at least in vitro, was explored in a different approach, which is described below.

CAPN3 Fragments Separately Translated in Vitro Undergo iMOC and Proteolyze CAST in a Na⁺-Dependent Manner.

To further determine whether CAST is a differential substrate for FL- and iMOC-CAPN3, an in vitro translation (IVT) system using wheat germ extract, in which cotranslation guarantees 100% coexpression of proteins, was used to produce the autolytic fragments of CAPN3. When the complementary fragments of CAPN3 were cotranslated, the interaction between N_{31K} or N_{31K}:C > S and C_{58K}, was detected. The resulting autolytic activity was found to be dependent on the active-site Cys aar, confirming the results of the COS7 cell experiment (Fig. 4A). In addition, it was demonstrated that CAST is more efficiently proteolyzed by FL-CAPN3 than iMOC-CAPN3 (Fig. S5 B and C).

The proteolysis of CAST was also assayed using a Cy3-labeled domain 1 fragment of CAST (Fig. 4B, Cy3-cast-d1). Because the cotranslation of iMOC-CAPN3 resulted in significant autolysis (Fig. 4A, lane 3), separately translated CAPN3 fragments were mixed immediately before their incubation with Cy3-cast-d1 (Fig. 4B). In the presence of 5 mM EDTA/K, which was sufficient to inhibit the translation reaction (Fig. S5D), cast-d1’s proteolysis was detected in the FL and iMOC samples, but not in the iMOC_{C>S} sample (Fig. 4C, lanes 2 and 5 vs. lane 8). Consistent with the fact that CAPN3 is a Na⁺-dependent protease (35), these activities were accelerated by the presence of 0.1 M NaCl (Fig. 4C, lanes 3 and 6 vs. lane 9). Under these conditions, the autolysis of CAPN3 also proceeded in both the FL and WT iMOC samples (Fig. 4C,

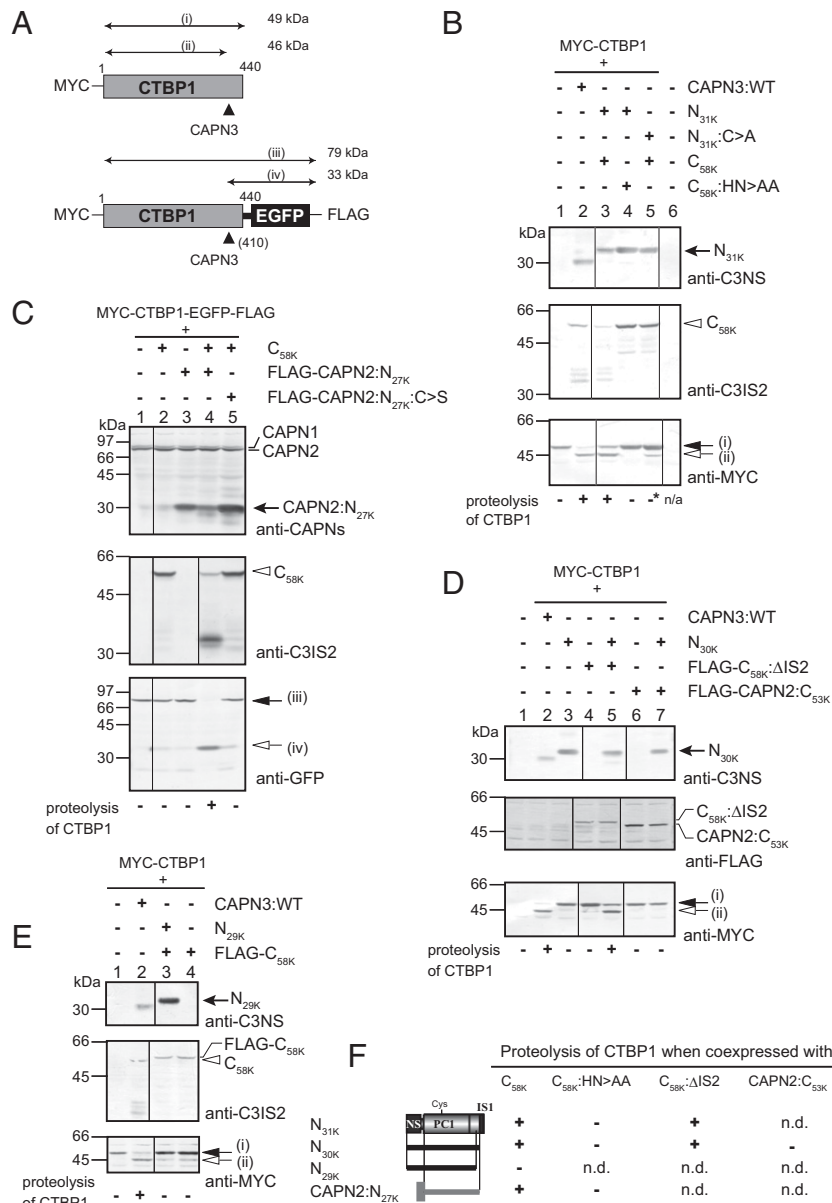


Fig. 2. CAPN3 protease activity is reconstituted by iMOC between autolytic fragments. (A) Two constructs of CTBP1 were used to generate substrates for monitoring the protease activity of CAPN3. Bidirectional arrows indicate the fragments detected by antibodies. Bidirectional arrows (i) and (ii) show segments detected by anti-MYC before and after proteolysis; (iii) and (iv) show segments detected by anti-FLAG before and after proteolysis. (B) MYC-CTBP1 was coexpressed with various CAPN3 constructs in COS7 cells. A proteolytic fragment of CTBP1 (A) was detected when CAPN3:WT was expressed [lane 2, anti-MYC (ii)]. The combination of N_{31K} and C_{58K} also caused CTBP1 proteolysis (lane 3). Comparison of two theoretically inactive combinations, N_{31K} and C_{58K}:HN > AA (lane 4), and N_{31K}:C > S and C_{58K} (lane 5), indicated that endogenous COS7 protein(s) may compensate for the function of N_{31K} in complementing C_{58K} (*), but not vice versa. Decreased amount of N_{31K} and C_{58K} in lane 3 suggests that iMOC between the fragments leads to their proteolysis. Arrow and open arrowhead indicate the N-terminal (N_{31K}) and the C-terminal (C_{58K}) fragments of CAPN3. (C) The N-terminal region of CAPN2, CAPN2:N_{27K}, corresponding to N_{30K}, was able to substitute for N_{31K} in iMOC with C_{58K}. CTBP1 proteolysis was evaluated using the MYC-CTBP1-EGFP-FLAG construct (lane 4, anti-GFP). In the same sample, decreased amounts of CAPN2:N_{27K} and C_{58K} were also observed. (D) The combined expression of N_{30K} and C_{58K}:ΔIS2 led to the iMOC-induced proteolysis of MYC-CTBP1 (lane 5 vs. lanes 3 and 4). CAPN2:C_{53K} was unable to substitute for C_{58K}:ΔIS2 (lane 7). (E) Deletion of the C-terminal 7 aars from N_{30K}, in N_{29K}, abrogated its ability to complement C_{58K}, as assessed by MYC-CTBP1 proteolysis (lane 3). (F) Proteolytic activity generated by the various combinations of N- and C-terminal fragments from CAPN3 and CAPN2 are summarized. The NS, IS1, and IS2 domains were not required for the autolytic fragment-mediated iMOC. The N- but not the C-terminal fragment derived from CAPN2 was able to replace the corresponding region of CAPN3. n.d., not done. Open arrowhead indicates the C_{58K} fragment generated by autolysis. Thick arrows indicate the position of the expressed N-terminal fragment. Arrows in *i-iv* indicate the CTBP1 fragments shown in **A**.

lanes 2, 3, 5, and 6), but not in the iMOC_{C>S} samples (Fig. 4C, lanes 8 and 9). These results demonstrated that iMOC-CAPN3 retained the characteristics of FL-CAPN3, including the proteolysis of CAST, autolytic activity, and the propensity for increased proteolysis in the presence of Na⁺.

N- and C-Terminal Autolytic Fragments of CAPN3 Are Not Targeted to Myofibrils. In transient expression experiments using primary skeletal myotube cultures, CAPN3 is found to be predominantly localized to the sarcomeric M-line region (12). To examine the effect of autolysis on cellular localization, the N- and C-terminal autolyzed

Transfection	WT	Mut (Protease-inactive)	Mut/WT ratio (pep no.)		
			CAPN3	CTBP1	CAST
(I) FL-CAPN3 + MYC-CTBP1	CAPN3:WT	FL:SHN	9.78 (30)	4.45 (104)	1.61 (5)
(II) iMOC-CAPN3 + MYC-CTBP1	N _{31K} + C _{58K}	N _{31K} :C>A + C _{58K} :HN>AA	4.04 (15)	3.48 (100)	1.14 (5)

Fig. 3. Autolysis is the major proteolytic event in COS7 cells expressing iMOC-CAPN3. Proteomic analyses of COS7 cells expressing CAPN3 were performed on two different experimental sets. In each set, protein expression was compared between cells expressing either WT or inactive mutant (Mut) CAPN3. As a protease-inactive control for FL-CAPN3, FL:SHN has been sufficient; however, for the iMOC-CAPN3, all three catalytic amino acids were replaced with Ala to minimize nonspecific activity. The experimental procedure is also schematically shown in Fig. S6. pep no., number of peptides with a confidence level >95%.

fragments were expressed as GFP fusion and FLAG-tagged proteins, respectively, in primary myotubes. Remarkably, the results indicated that neither of the fragments retained the M-line localization characteristic of FL-CAPN3 (Fig. 5*A* and *B*, *iv* vs. *ii*), suggesting that upon autolysis, CAPN3 may localize to the cytosol for functions distinct from that of FL-CAPN3 by undergoing iMOC.

iMOC Mediated by Mutant FL-CAPN3 and Wild-Type Autolytic Fragments Rescues CAPN3's Autolytic Activity. During the course of these studies, to our surprise, a protease-inactive mutant of CAPN3, FL:AHN, was found to undergo proteolysis when coexpressed with N_{31K}, but not N_{31K}:C > S (Fig. 6*A*, lane 2 vs. lanes 1 and 3, gray arrowhead). However, the coexpression of N_{31K} with FL:AAA, another protease-inactive mutant in which all three catalytic amino acid residues were replaced with Ala, did not lead to the generation of proteolytic fragments (lane 5). These results demonstrate that the autolytic activity of CAPN3 was restored by iMOC between C129 in N_{31K} and H334/N358 in the FL molecule.

In the iMOC-mediated FL autolytic reaction observed above, N_{30K} was competent to substitute for N_{31K} (Fig. 6*B*, lanes 3 and 4), as in the case of iMOC mediated by two autolytic fragments. Furthermore, CAPN2:N_{27K} could also restore CAPN3 FL:SHN autolytic activity, in a CAPN2 Cys105-dependent manner (Fig. 6*C*, lane 4 vs. lane 5). Notably, the mutations D120A/E199A present in N_{31K}:DE > AA abrogated the iMOC-mediated autolysis

(Fig. 6*B*, lane 6). These amino acid residues correspond to the Ca²⁺-binding site in PC1 (CBS1) in CAPN1 and CAPN2 and were shown to be involved in the Na⁺ responsiveness of CAPN3 (35).

The proteolytic product generated from FL:AHN (or FL:SHN) following iMOC with N-terminal competent fragments and detected by anti-C3IS2 antibodies, appeared to be identical to the C_{58K} fragment (Fig. 6*A–D*, gray arrowhead, anti-C3IS2). When a C-terminal 27-aa truncation was introduced into FL:AHN (FL:AHN:ΔC27; Fig. 1*A*), the proteolytic fragment generated from this mutant following coexpression with either CAPN3:WT or N_{30K} exhibited a reduction in molecular weight by ~27 aars (Fig. 6*D*, lanes 1 and 2 vs. lanes 5 and 6, open arrow). Thus, the 58-kDa product generated from FL:AHN by iMOC-mediated autolysis likely represented the C-terminal fragment, identical to C_{58K} produced by the canonical autolysis of CAPN3:WT. The N-terminal proteolytic products generated from FL:AHN had sizes close to N_{31K}; these fragments are supposed to be competent for iMOC if not for the C129A mutation (Fig. 6*B*, lanes 3 and 4, bracket).

Notably, the lack of autolytic activity associated with FL:CAA was rescued by C_{58K} (Fig. S1*C*, lane 10), but not by C_{58K}:HN > AA (lane 11). These results indicate that the coexpression of a CAPN3 mutant and the appropriate N- or C-terminal autolytic fragment (for example, FL-CAPN3 with a mutation at the N terminus + N-terminal fragment without a mutation), results in a protease activity similar to that of iMOC-CAPN3.

IS1 and IS2 in the FL-CAPN3 Are Required for iMOC-Mediated FL Autolysis. Next, the role of the CAPN3-specific sequences (NS, IS1, and IS2) in FL-CAPN3-mediated iMOC was assessed using a series of deletion mutants in which the active-site Cys was replaced by Ser (for mutants, see Fig. 1*A*). The mutant FL:SHN:ΔNS, which was recognized as a substrate for CAPN3:WT, was found to undergo iMOC with N_{30K} or N_{31K}, resulting in the generation of autolytic fragments (Fig. 7*A*, lanes 3 and 5 vs. lane 4), indicating that the NS in FL-CAPN3 is dispensable for iMOC with the N-terminal autolytic fragments of CAPN3. On the other hand, coexpression of the IS1 deletion mutant FL:SHN:ΔIS1 with either N_{30K} or N_{31K} did not result in production of the proteolytic C_{58K} fragment (Fig. 7*B*, lanes 3–5). This result indicates that, like

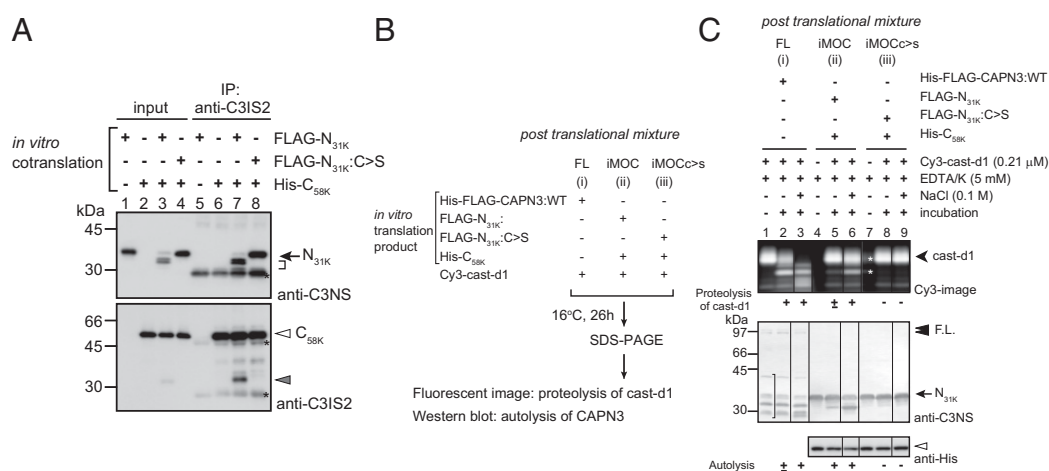


Fig. 4. In vitro translated CAPN3 fragments form active protease complexes de novo. (A) iMOC mediated by in vitro translated fragments of CAPN3. Cotranslation of the CAPN3 fragments N_{31K} and C_{58K} produced autolytic activity (lane 3 vs. lanes 1, 2, and 4; bracket and gray arrowhead). Both N_{31K} and N_{31K}:C > S were coimmunoprecipitated with the C_{58K} fragment using the anti-C3IS2 antibody (lanes 7 and 8, anti-C3NS). Autolytic fragments of N_{31K} were also detected in the immunoprecipitant (lane 7, bracket). *Nonspecific signal. (B) Posttranslational formation of iMOC-CAPN3. Separately translated products were mixed, and the proteolytic activity was evaluated using Cy3-labeled cast-d1 as a substrate. (C) Proteolysis of Cy3-cast-d1 was detected in the FL (*i*) or iMOC (*ii*), but not in the iMOC_{c>s} reaction (*iii*) (Cy3-image, lanes 2 and 5 vs. lane 8). In both *i* and *ii*, cast-d1 proteolysis and CAPN3 autolysis was increased in the presence of Na⁺ (lanes 3 and 6 vs. lane 8). A total of 5 mM EDTA/K inhibits translation; thus, translation during the iMOC incubation was considered to be negligible. *Carry over from the adjacent lane (lane 7).

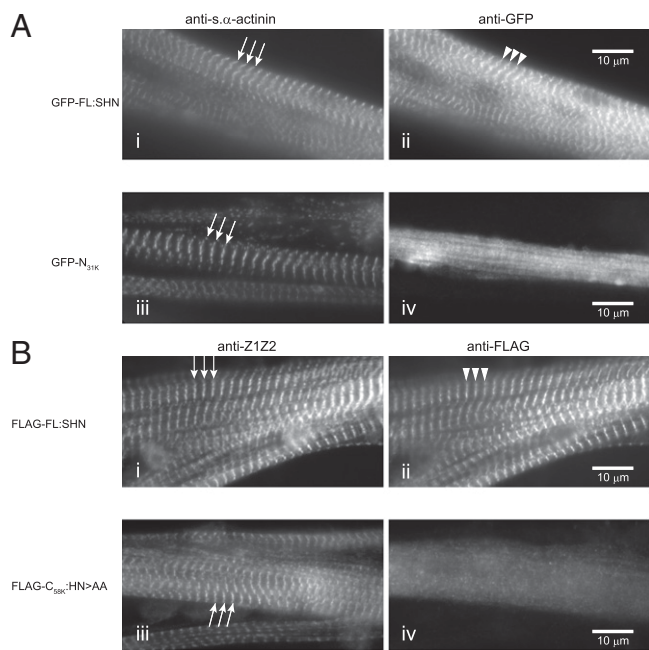


Fig. 5. Altered subcellular localization of N_{31K} and C_{58K} in myotubes compared with FL-CAPN3. N_{31K} and C_{58K} :HN > AA expressed in primary chick skeletal myotubes showed a diffuse localization, distinct from the striated M-line localization of CAPN3 FL:SHN (A and B, iv vs. ii). Arrows indicate Z-lines labeled by α -actinin or the N terminus of titin/connectin (Z1-Z2). Arrowheads indicate the striated localization of FL:SHN, visualized by anti-GFP or anti-FLAG antibodies. (Scale bars, 10 μ m.)

the canonical autolysis of FL-CAPN3, the IS1 sequence is required for CAPN3 to undergo iMOC-mediated autolysis.

FL:SHN: Δ IS2 was capable of serving as a substrate for CAPN3:WT, as the coexpression of these two CAPN3 forms resulted in the generation of a proteolytic fragment corresponding to the IS2-deleted form of C_{58K} (C_{58K} : Δ IS2) (Fig. 7C, lane 2). In contrast, C_{58K} : Δ IS2 was not observed when FL:SHN: Δ IS2 was coexpressed with N_{31K} or N_{30K} (Fig. 7C, lanes 3 and 4), indicating a failure of these fragments to undergo iMOC leading to autolysis. In addition, FL:SHN: Δ IS2 was unable to cooperate with N_{31K} or N_{30K} to proteolyze CTBP1, unlike N_{30K} + C_{58K} : Δ IS2 (Fig. 7C, lanes 3 and 4 vs. Fig. 2C, anti-MYC, lane 5). Taken together, these results indicate that both IS1 and IS2 in the FL-CAPN3 are required for the iMOC-mediated autolysis of inactive FL-CAPN3 (Fig. 7D).

Discussion

“Complementation” refers to a phenomenon in which functional activity is restored through the noncovalent interaction of two (or more) different proteins, as in the case of α -complementation in *Escherichia coli* β -galactosidase, in which the α -fragment and ω -fragment of this enzyme restore enzymatic activity when expressed *in trans* (36, 37). In addition, it has been demonstrated that physiological functions of some proteins including membrane receptors and enzymes are mediated by intermolecular complementation (38–41). In the present study, we showed that autolyzed fragments of CAPN3, neither of which has protease activity when expressed alone, complement each other to reconstitute protease activity in a manner similar to α -complementation. Our data also strongly support and provide a molecular mechanism for the hybrid hypothesis (34), a model based on the finding that patients with LGMD2A exhibiting compound heterozygous mutations in different domains of CAPN3 may show reduced pathology compared with patients with single homozygous mutations (Fig. 1B). In this model, two complementary fragments generated from different

CAPN3 molecules form an active protease complex by sharing active-site amino acid residues in each fragment. One of the remarkable aspects of CAPN3 is that the complementary complex can be formed spontaneously from separately generated fragments *de novo*. To our knowledge, such a property has only been reported for pPR, a protease in cytomegalovirus (41), which is described below.

Intriguingly, the initial autolytic cleavage of CAPN3 requires the CAPN3-specific sequences IS1 and IS2 (11, 42), whereas these sites are dispensable for the iMOC of autolyzed fragments. In addition, as CAPN2: N_{27K} can replace CAPN3 N_{30K} in the fragment-based iMOC, it is tempting to predict that many, if not all of the CAPNs could potentially undergo iMOC (Fig. 2C and Fig. S3). In fact, CAPN1 and CAPN9 have 3D structures (43)

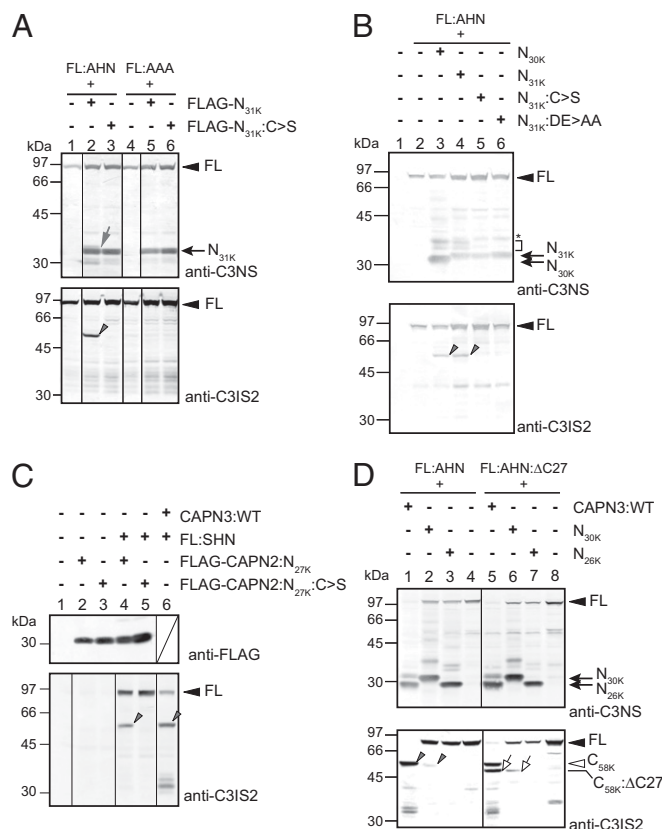


Fig. 6. The N-terminal autolytic fragment of CAPN3 restores the autolytic activity of inactive mutant CAPN3 through iMOC. (A) When expressed in COS7 cells, FL:AHN, a catalytically inactive mutant, failed to undergo autolysis (lane 1). Coexpression of N_{31K} with FL:AHN generated a fragment with a similar mobility to the C_{58K} fragment and trace amounts of N-terminal fragment (lane 2, gray arrow). These fragments were not detected when N_{31K} was replaced by N_{31K} :C > S (lane 3) or when FL:AHN was replaced by FL:AAA (lanes 4–6), a catalytically inactive mutant in which all three active site residues were replaced by Ala. (B) Deletion of the IS1 region from N_{31K} in N_{30K} did not affect iMOC-mediated autolysis of FL:AHN (lane 3 vs. lane 4, gray arrowhead). However, the autolytic reaction was compromised by Ca^{2+} binding-site mutations in the PC1 domain of N_{31K} (lane 5 vs. lane 6). (C) The N-terminal region of CAPN2, CAPN2: N_{27K} , could substitute for N_{30K} or N_{31K} in generating the C_{58K} -like fragment from FL:SHN (lane 4, gray arrowhead). The active-site Cys105 in CAPN2 was required for the reaction (lane 5). (D) The C_{58K} fragment generated from FL:AHN by CAPN3:WT was reduced in size by introducing a C-terminal truncation, FL:AHN: Δ C27 (lane 1 vs. lane 5). A similar change in product size was observed after the coexpression of FL:AHN: Δ C27 with N_{30K} (lane 2 vs. lane 6). Arrowhead and open arrowhead indicate the full-length (FL) product of the protease-inactive CAPN3 mutants and the C_{58K} fragment, respectively. Open and closed arrows indicate the positions of the 27-aa truncated C_{58K} generated from FL:AHN: Δ C27 and the expressed N-terminal fragment, respectively.

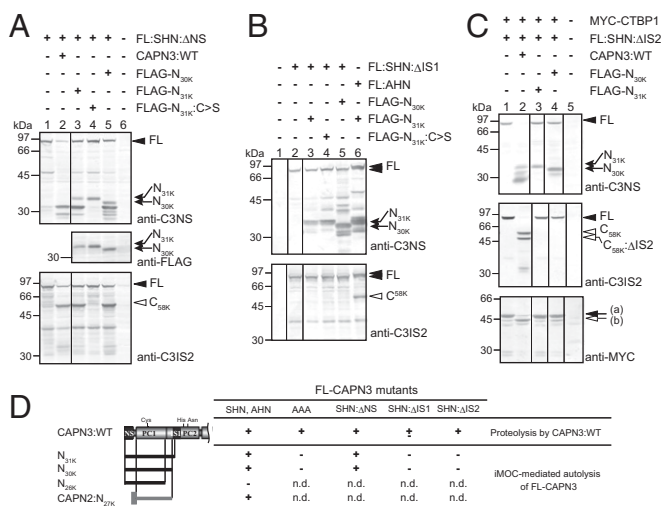


Fig. 7. The CAPN3-specific insertion sequences IS1 and IS2 are required for the iMOC-mediated autolysis of FL-CAPN3. (A) The protease-inactive deletion mutant FL:SHN:ΔNS was coexpressed with CAPN3:WT or the N-terminal fragments in COS7 cells. In addition to CAPN3:WT, both N_{30K} and N_{31K} were able to generate the C_{58K} autolytic fragment from FL:SHN:ΔNS (lanes 3 and 5 vs. lane 2, open arrow). The autolytic fragment was not generated when N_{31K} was replaced with N_{31K}:C>S (lane 4). (B) Coexpression of FL:SHN:ΔIS1 with N_{31K} or N_{30K} did not result in the generation of the C_{58K} autolytic fragment (lanes 3 and 5 vs. lane 6). (C) Coexpression of FL:SHN:ΔIS2 with CAPN3:WT generated a slightly smaller fragment than C_{58K} (lane 2, lower open arrowhead, C_{58K}:ΔIS2), which was not generated when N_{31K} or N_{30K} was substituted for CAPN3:WT (lanes 3 and 4). Similarly, CTBP1's proteolysis was undetectable when N_{31K} or N_{30K} was coexpressed with FL:SHN:ΔIS2 [anti-MYC; lanes 3 and 4 vs. lane 2 (B)]. (D) The effects of deleting NS, IS1, or IS2 on iMOC-mediated autolysis are summarized. The lack of either IS1 or IS2 abrogated iMOC-mediated autolysis of FL-CAPN3. Note that the ability of CAPN3 to serve as a substrate for CAPN3:WT did not depend on IS2.

similar to that of CAPN2 in the region of PC2 containing β1, α1, and β2, which are thought to be crucial for iMOC. From physiological aspect, however, such iMOC compatibility may not be relevant. As of now, it is assumed that most CAPNs do not spontaneously undergo autolysis to generate the fragments corresponding to N_{31K} and C_{58K} of CAPN3. In addition, the calpain species that never coexist with CAPN3 in skeletal muscle have no chance to be involved in complementation with CAPN3 fragments.

It should also be noted that there is no evidence that ubiquitous calpains expressed in skeletal muscle complement CAPN3's function. This could be due to the fact that the physiologically essential characteristic of CAPN3, such as its sensitivity to Ca²⁺ or Na⁺ as well as cellular localization, is not complemented by the fragment from other calpain species.

Consistent with the above notion, in contrast to CAPN2:N_{27K}, CAPN2:C_{53K} was not functionally equivalent to the corresponding CAPN3 fragment, C_{58K}. Thus, this region of CAPN3 appears to encode the functional specificity for iMOC (Fig. S2B). The specific feature(s) in the C-terminal region of CAPN3 that distinguish it from that of CAPN2 is currently unclear. Previous findings indicate that both CAPN1 and CAPN2 can form a heterodimer with the calpain small subunit (CAPNS1) via the PEF(L) domain. However, a similar heterodimer of CAPN3 with CAPNS1 has not been detected, which may also suggest that the carboxyl-terminal region of CAPN3 and other CAPNs plays different roles in these related proteases. In line with such difference, the EF5-hand of CAPN3 is unique in that it is a binding site for Ca²⁺ as well as an interacting site for homodimer formation of the PEF(L) domain (33). It was also shown that a CAPN3 mutant completely lacking IS2 and PEF(L) (CAPN3: S581X), expresses protease activity comparable to that of FL-CAPN3

(35). Further studies will be required to elucidate the precise role of the carboxyl-terminal region in regulating CAPN3's autolysis and the function of iMOC.

The rescue of inactive FL-CAPN3 involves iMOC mediated by either the N- or C-terminal autolytic fragment (Fig. 8A and Fig. 8B). The N-terminal fragment-mediated iMOC provided the active-site Cys, whereas both the NS and IS1 domains were dispensable. On the other hand, the presence of both IS2 and IS1 were required in the FL-CAPN3 mutant for the iMOC-mediated restoration of activity. The effect of the ΔIS1 mutation was expected, as it compromises the structure of the CAPN3 autolytic sites. Because IS2 plays a role in the Ca²⁺-independent activity of CAPN3 (11, 35), its deletion may change the structure of PC2. However, we demonstrated that the IS2 in C_{58K} was not required for the formation of the active CysPc through iMOC with the FL:CAA mutant (Fig. 8B and Fig. 8C). Therefore, IS2 was required in FL-CAPN3, but not in C_{58K}. Although the stoichiometry of the N- or C-terminal fragment and FL-CAPN3 in the iMOC complex is not clear, the CysPc domain in CAPN3 somehow circumvents steric hindrance by the extra PC1 or PC2 domains, probably via flexibility introduced by IS1.

The homodimer formation of CAPN3 may have a certain role in iMOC (34). In the modeled structure of the FL-CAPN3 homodimer, protease core domains of two monomers are located at the outside of the complex, far from the interface (32). Therefore, it is not necessarily a monomer form of CAPN3 that performs iMOC. For example, iMOC may be more efficient for the autolytic fragments generated from different CAPN3 LGMD2A mutants in the same dimer. Alternatively, a dimer of FL-CAPN3 and/or C_{58K} may have a structural advantage to perform iMOC with N_{31K}. The molecular mechanism involved in CAPN3 iMOC will be an interesting area of investigation for structural biologists.

The critical difference between CAPN3 iMOC and the complementation of β-galactosidase is that CAPN3 innately generates the complementary fragments as natural products of autolysis. Such a mechanism coupling autolysis and complementation for the restoration of protease activity has been well studied for a capsid scaffold protein that functions as a capsid maturational protease (pPR, pUL80a) in cytomegalovirus (CMV) (41). During the course of viral capsid maturation, pPR functions as a critical protease in three forms: pPR, assemblin, and the reconstituted form of assemblin autolyzed products. Although the different forms of pPR may share the same substrate specificity, changes in its molecular size and conformation are necessary for its roles in maintaining efficient viral reproduction and for the removal of scaffold proteins from the capsid before incorporation of the viral DNA (44, 45). Interestingly, the fragments artificially generated from the assemblin homolog in HSV type I has the potential to undergo iMOC, but, such fragments are not naturally generated by autolysis (46, 47); it is attributed to the fact that HSV assemblin does not have an autolytic sequence corresponding to the one found in CMV assemblin (48). It has also been suggested that the difference in the functionality of two closely related assemblin homologs may reflect certain physical constraints, such as the size of the capsid and viral genome in each species.

FL-CAPN3 was previously shown to be most stably expressed in the myofibril-bound fraction of skeletal muscle cells (15). FL-CAPN3 is hypothesized to be highly regulated, requiring induction by certain biological conditions. The iMOC-induced activation of CAPN3 revealed in the present study suggests an alternative pathway for expressing CAPN3 activity (Fig. 8). In analogy to pPR, we hypothesize that the iMOC form may have greater mobility than FL-CAPN3 within skeletal muscle cells, which are densely packed with myofibril components (49). The observation that transiently expressed autolyzed fragments were found to be diffusely distributed in skeletal muscle cells instead of localizing to the sarcomeric M-line region (Fig. 5) supports this hypothesis in part. Reassembly of two fragments, however, is required to form an

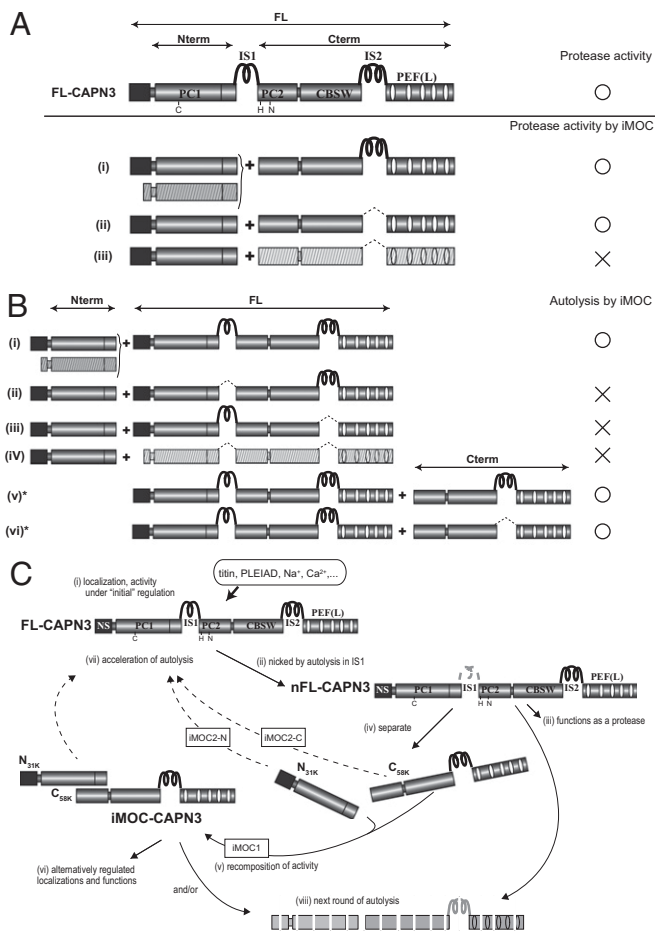


Fig. 8. iMOC contributes to the previously unidentified regulation of CAPN3. (A) The FL-CAPN3 is an active protease (diagram at Top). Through autolysis, it is converted into two fragments, designated Nterm and Cterm, which flank the ISI region (*i–iii*). The iMOC-mediated reconstitution of protease activity requires the coexpression of complementary Nterm and Cterm fragments. The N-terminal fragment of CAPN3 can be replaced by the corresponding region in CAPN2 (*i*). Although the C-terminal IS2 region is not required for iMOC-mediated autolysis, the C-terminal region of CAPN2 is unable to substitute for CAPN3 Cterm (*ii* and *iii*). Shaded box indicates that the construct is derived from CAPN2. (B) iMOC between Nterm and inactive FL-CAPN3 mutants restores autolytic activity (*i*) and requires the presence of both IS1 and IS2 (*ii–iv*). The Cterm, C_{58K}, also undergoes iMOC with FL-CAPN3 mutants, restoring autolytic activity (*v*), but does not require IS2 in the Cterm (*vi*). *The results are shown in Fig. S1C. (C) Revised model of the CAPN3 autolytic cycle. In this model, autolysis is viewed as both a positive and negative regulator of CAPN3 function. The preautolytic FL-CAPN3 is regulated by previously identified factors (*i*). Initially, autolysis leads to nicking in ISI (*ii*), resulting in the formation of nFL-CAPN3, allowing it to function as a protease (*iii*). The N- and C-terminal fragments separate (*iv*) and undergo iMOC (*v*), possibly involving additional regulatory mechanisms. After iMOC, the reconstituted CAPN3 may be alternatively regulated and take on additional functions (*vi*). At the same time, each autolytic fragment is capable of accelerating the autolysis of FL-CAPN3 by chimeric iMOC (iMOC2-N and iMOC2-C) (*vii*). The initial autolytic reaction is also accelerated by iMOC-CAPN3 (*viii*). The second round of autolysis is probably linked to the efficient down-regulation of CAPN3 (*viii*).

active enzyme, which may cause further kinetic and spatiotemporal constraint for function. In this regard, the overall kinetics of CAPN3 should be further investigated together with its interacting molecules through the process of autolysis to iMOC formation.

Our proteomic analysis showed that both FL- and iMOC-CAPN3 exhibited substantial autolytic activity. This property of iMOC-CAPN3 is consistent with the finding that the autolysis of

CAPN3 was maintained by its autolytic products and may explain the exhaustiveness of CAPN3's autolysis. We also found that CAST is more efficiently proteolyzed by FL-CAPN3 than by iMOC-CAPN3 in ectopic protein expression systems. Although it is still an open question whether there are physiologically significant differences in substrate specificity between FL-CAPN3 and iMOC-CAPN3, they have different sensitivity to inhibitors (Fig. S64) (27). Considering that FL-CAPN3's autolysis is very rapid, CAPN3 nicked by autolysis (nFL-CAPN3) (Fig. 8C) must be somewhat stable, requiring time to separate into fragments (27–29). It is currently unknown whether the preautolytic FL-CAPN3 proteolyzes other substrates before it is converted to nFL-CAPN3, or whether FL- and nFL-CAPN3 have distinct substrate preferences.

The present study revealed that autolyzed fragments of CAPN3 generate *de novo* protease activity via iMOC. This finding provides a possible molecular mechanism for the functional compensation between two distinct CAPN3 molecules (Fig. 1B). Therefore, at least three active molecular states of CAPN3 can be distinguished as shown in Fig. 8C; FL-CAPN3, nFL-CAPN3, and iMOC-CAPN3. Further studies should enhance our understanding of the mechanism by which CAPN3 exerts its protease activity and extend our understanding of the genotype–phenotype relationship in LGMD2A, as well as the molecular mechanisms underlying the pathology of this disease.

Materials and Methods

cDNA Constructs. For protein expression in mammalian cells, cDNAs were subcloned into the pSRD expression vector, as described previously (16). The pEGFP-C1 and pcDNA3.1 (Invitrogen) expression vectors were used for protein expression in chick skeletal myotubes (16). For *in vitro* transcription and translation, the human CAPN3 cDNAs were subcloned into the pEU-E01 vector (CellFree Sciences) (50). Where indicated, the proteins were expressed as MYC-, FLAG-, or His-tagged forms. Enzymes used for manipulating recombinant DNA were purchased from Takara Bio, Iwai Chemicals, New England Biolabs, and Agilent Technologies. The mutations described here were introduced by long PCR using PfuTurbo DNA polymerase, as described previously (26). The sequences of all of the constructs were verified.

Cell Culture and Protein Expression. Proteins were expressed in COS7 cells as previously described (16). COS7 cells were grown in DMEM (Sigma-Aldrich) supplemented with 10% (vol/vol) FBS that was heat inactivated at 56 °C for 30 min before use. The cells metabolically labeled using SILAC Protein Quantitation kit (Pierce) were also used for protein expression. Plasmid prepared at a concentration of 1 μg/μL was transfected into cells using TransIT-LT1 (Mirus Bio), according to the manufacturer's instructions. For each transfection, 1.2–1.5 × 10⁵ cells were seeded in a 3.5-cm dish 12–16 h before transfection, and 1 μg of plasmid per construct was used as the standard condition. The cells were harvested 48–60 h after transfection using ice-cold PBS, resuspended in sonication buffer [20 mM Tris-Cl, pH 7.5, 1 mM EDTA-K, pH 8.0, 1 mM DTT, 2 mM 4-(2-aminoethyl) benzenesulfonyl fluoride hydrochloride (AEBSF)], and lysed by sonication. For proteomic analysis, the cell lysate was prepared in 20 mM triethylammonium bicarbonate containing 20 μM ALLNaI (Sigma-Aldrich) and 20 μM calpeptin (Calbiochem) and subjected to sonication and centrifugation at 18,000 × *g* for 20 min at 4 °C (51). Protein concentration was quantified using the DC protein assay (Bio-Rad) or Direct Detect (Merck).

In Vitro Transcription and Translation. *In vitro* transcription and translation were performed using the wheat-germ cell-free expression system according to the manufacturer's instructions (CellFree Sciences) (50). The mRNAs for each construct were separately transcribed. The translation reaction was carried out at 16 °C for 18–20 h without shaking. For the coexpression of CAPN3 fragments, an equal volume of transcription product for each construct was mixed before the translation reaction. The volume of the translation reaction was adjusted to 30–100 μL, maintaining the ratio of constituents as indicated in the instructions. Where indicated, the translation reaction was carried out in the presence of protease inhibitors.

Western Blot Analysis. Proteins were separated by SDS/PAGE and transferred onto PVDF membranes (Millipore). The membranes were probed with appropriate primary antibodies and horseradish peroxidase-coupled secondary antibodies (Nichirei) followed by visualization using a POD immunostaining

kit (Wako) or the Clarity Western ECL Substrate (Bio-Rad). Chemiluminescence signals were detected by the ImageQuant LAS 4000 imaging system (GE Healthcare). Scanned images were processed for presentation using Adobe Photoshop CS6 (Adobe Systems).

Immunoprecipitation. In vitro translation reaction mixtures were diluted in a 10- to 15-fold excess volume of lysis buffer (50 mM Tris-HCl, pH 7.5, 150 mM CsCl, 1 mM EDTA-K, pH 8.0, 1% Triton X-100, 1 mM AEBSF, 0.1 mM leupeptin, 10 μ g/mL aprotinin, and 10 mM iodoacetamide) (52), and incubated on ice for 30 min with occasional mixing. The supernatant was collected after centrifugation at 20,630 \times g for 5 min at 4 $^{\circ}$ C. Preabsorption of nonspecific interactions was performed using Protein-G Sepharose (GE Healthcare). Subsequently, the supernatant was incubated with goat anti-C3IS2 IgG (29) for 8–12 h, followed by the precipitation of immunocomplexes with Protein-G Sepharose according to the manufacturer's instructions. Precipitated immunocomplexes were washed twice with lysis buffer and twice with a wash buffer that was modified from its previous description (50 mM Tris-HCl, pH 7.5, 150 mM CsCl). Immunoprecipitated proteins were denatured in SDS/PAGE sample buffer and subjected to SDS/PAGE. Immunoprecipitation using anti-FLAG M2 affinity gel (Sigma-Aldrich) was performed as described (52). The same protocol was used for the immunoprecipitation of proteins expressed in COS7 cells; cells collected from one dish were lysed in 1 mL of lysis buffer.

Immunofluorescence Analysis. The transfection of primary chick skeletal myotubes and immunofluorescence microscopy were performed as described previously (53). Briefly, transfection was performed using Effectene (Qiagen). Six days later the transfected myotubes were incubated in relaxing buffer (150 mM KCl, 5 mM MgCl₂, 10 mM 3-(*N*-morpholino) propanesulfonic acid, pH 7.4, 1 mM EGTA, and 4 mM ATP) for 15 min, then fixed with 2% (wt/vol) formaldehyde in relaxing buffer for 15 min. The primary and the secondary antibodies were used at concentrations described below. Coverslips were mounted onto slides with Aqua Poly/Mount (Polysciences) and analyzed on an Axiovert microscope (Zeiss, Oberkochen) using 63 \times (NA 1.4) or 100 \times (NA 1.3) objectives. The images were processed for presentation using Adobe Photoshop CS6 (Adobe Systems).

Antibodies. The antibodies used in this study included anti-FLAG mouse monoclonal antibody (1:1,000; M2, Stratagene), anti-MYC mouse monoclonal antibody (1:1,000; 9E10, Developmental Studies Hybridoma Bank), anti-GFP rabbit polyclonal antibody (1:2,000; Abcam, and 1:1,000; mFX75, Wako), anti-CAPN3 IS2 goat polyclonal antibody (1:1,000, Cosmo Bio (designated as anti-C3IS2)), anti-CAPN3 rabbit polyclonal antibodies (1:1,000; RP4-Calpain3, Triple Point Biologics (designated as anti-C3NS), and 1:400; anti-CAPN3-1, Myomedix (designated as anti-CAPN3)), anti-His mouse monoclonal antibody (1:1,000; His-Tag, Novagen), antisarcomeric- α -actinin mouse monoclonal antibody (1:15,000; EA53, Sigma-Aldrich), and antititin Z1-Z2 rabbit polyclonal antibody (1:100) (53). Mouse monoclonal pan calpain antibody (anti-CAPNs) was kindly provided by Seiichi Kawashima (Tokyo Metropolitan Institute of Medical Science, Tokyo).

Calpastatin Proteolytic Assay. All procedures were performed under light-protected conditions. Cast-d1 (Takara Bio) was labeled using Cy3 mono-reactive dye (GE Healthcare) according to the manufacturer's instructions with some modifications. The labeling reaction was stopped by adding lysine at a final concentration of 20 mM, and labeled protein was purified using a PD SpinTrap G25 column (GE Healthcare). Thirty nanograms (2.1 pmol) of labeled cast-d1 was incubated with 4 μ L of in vitro translation (IVT) reaction mixture in a total volume of 10 μ L at 16 $^{\circ}$ C for 26 h. The final composition of the incubation solution was 20 mM Tris-HCl, pH 7.5, 1 mM EDTA/K, 1 mM DTT, 2 mM AEBSF, and either 5 mM EDTA/K or 0.1 M NaCl. The reaction was stopped by the addition of SDS sample buffer, and the sample was subjected to SDS/PAGE. Fluorescent signals were detected using Typhoon 9400 laser scanner (GE Healthcare), followed by image processing using Adobe Photoshop CS6 (Adobe Systems). The same gel was used for Western blot analysis.

Proteomic Analysis. Two sets of experiments were performed (Fig. S6A). The cell lysate was prepared as described in *Cell Culture and Protein Expression*. For each sample group, 20 μ g of protein from each of two independent transfection procedures were combined, and a total of 40 μ g was processed according to the instructions in the iTRAQ 4-Plex Reagent kit (AB SCIEX). Ten micrograms each of endoprotease Lys-C (Wako) and trypsin (Promega) were used to digest 40 μ g of protein. The digests from each sample were divided into two equal portions for labeling with two different iTRAQ tags (Fig. S6A). After the labeling reaction, the peptides were mixed and then separated into three fractions, by eluting with 87.5 mM, 175 mM, and 350 mM KCl, using the ICAT Cation Exchange Buffer Pack (AB SCIEX). Each fraction was desalted using a Sep-Pak Light C18 cartridge (Waters) and concentrated by evaporation. MS/MS spectral data were acquired using the TripleTOF 5600⁺ system (AB SCIEX) equipped with a Nano LC Ultra 1D Plus system (Eksigent).

Protein Identification and Quantification. Proteins were identified and quantified using Protein Pilot (ver. 4.5, AB SCIEX). The Paragon algorithm in the Protein Pilot software was used as a search program with the following settings: trypsin digestion, methyl methanethiosulfonate modification of cysteines, iTRAQ 4-plex labeled peptides, instrument 5600, no special factors, default iTRAQ isotope correction settings, quantification, bias correction, background correction, biological modifications, amino acid substitutions, and thorough ID parameters selected. To improve the identification of protein from COS7 cells, which are established from monkey, the human database was manually supplemented with the sequences for other primates (UniProt database released in September 2012). This procedure increased the number of identified proteins by 2–3%, however, approximately 65% of identified proteins were found only in a human database (Fig. S6B). Inspection of identified proteins suggests that the sequence conservation between human and monkey is high enough for the search program with the settings we used (54). Therefore, it was concluded that the use of a human database for the present study is reasonable and necessary. In the two sets of experiments, 2,769 [(I) FL-CAPN3] and 3,169 [(II) iMOC-CAPN3] proteins were identified with a global false discovery rate (FDR) of <5% (Fig. S6B).

SILAC-Based Quantitation. The immunoprecipitated proteins from metabolically labeled COS7 cells were mixed 1:1 and digested using endoprotease Lys-C (Wako). After concentration and desalting, peptides were analyzed by the TripleTOF 5600⁺ system (AB SCIEX). Peptides and proteins were identified using Protein Pilot (ver. 4.5, AB SCIEX). Among the peptides with a confidence level of >95%, consistently modified peptides that are found in both light- and heavy-labeled forms are selected for quantitation. SILAC ratios (light:heavy) were calculated for the peak intensity of selected peptides using PeakView (ver. 2, AB SCIEX).

Sequence and Structure Analysis. Protein sequence data were retrieved from the UniProtKB or NCBI database. The sequences were aligned using MAFFT, and the result was processed using Genetyx (ver. 11) (Genetyx). To investigate the structure of the reconstituted protease domain of CAPN3, the crystal structure of the protease domain of rat CAPN2 in the presence of Ca²⁺ (Protein Data Bank 1MDW) (6) was used as a template. Using the MolFeat ver. 5 (FiatLux), the coordination of the two autolytic fragments of CAPN3 was modeled. The processed image was exported for further modification using Adobe Photoshop CS6 (Adobe Systems).

ACKNOWLEDGMENTS. We thank Drs. Amets Sáenz and Adolfo Lopez de Munain for their sincere interest in the genotype–phenotype relationships in LGMD2A, which prompted us to generate a novel, testable hypothesis, and all the Calpain Project laboratory members for their invaluable support. This work was supported in part by Japan Society for the Promotion of Science.KAKENHI Grants 20370055 and 23247021 (to H.S.), 22770139 and 25440059 (to Y.O.), a Takeda Science Foundation research grant (to H.S.), the Collaborative Research Program of the Institute for Chemical Research (Kyoto University) Grant 2010-15 (to H.S.), Grants 2011-18 and 2012-30 (to Y.O.), a Toray Science and Technology grant (to Y.O.), and National Institutes of Health Grants HL083146 and HL108625 (to C.C.G.).

1. Sorimachi H, et al. (1989) Molecular cloning of a novel mammalian calcium-dependent protease distinct from both m- and mu-types. Specific expression of the mRNA in skeletal muscle. *J Biol Chem* 264(33):20106–20111.
2. Goll DE, Thompson VF, Li H, Wei W, Cong J (2003) The calpain system. *Physiol Rev* 83(3):731–801.
3. Sorimachi H, Hata S, Ono Y (2011) Calpain chronicle—an enzyme family under multidisciplinary characterization. *Proc Jpn Acad, Ser B, Phys Biol Sci* 87(6): 287–327.

4. Sorimachi H, Hata S, Ono Y (2011) Impact of genetic insights into calpain biology. *J Biochem* 150(1):23–37.
5. Ono Y, Sorimachi H (2012) Calpains: An elaborate proteolytic system. *Biochim Biophys Acta* 1824(1):224–236.
6. Moldoveanu T, Hosfield CM, Lim D, Jia Z, Davies PL (2003) Calpain silencing by a reversible intrinsic mechanism. *Nat Struct Biol* 10(5):371–378.
7. Moldoveanu T, Jia Z, Davies PL (2004) Calpain activation by cooperative Ca²⁺ binding at two non-EF-hand sites. *J Biol Chem* 279(7):6106–6114.

8. Hanna RA, Campbell RL, Davies PL (2008) Calcium-bound structure of calpain and its mechanism of inhibition by calpastatin. *Nature* 456(7220):409–412.
9. Moldoveanu T, Gehring K, Green DR (2008) Concerted multi-pronged attack by calpastatin to occlude the catalytic cleft of heterodimeric calpains. *Nature* 456(7220):404–408.
10. Campbell RL, Davies PL (2012) Structure-function relationships in calpains. *Biochem J* 447(3):335–351.
11. Sorimachi H, et al. (1993) Muscle-specific calpain, p94, is degraded by autolysis immediately after translation, resulting in disappearance from muscle. *J Biol Chem* 268(14):10593–10605.
12. Ojima K, et al. (2007) Myogenic stage, sarcomere length, and protease activity modulate localization of muscle-specific calpain. *J Biol Chem* 282(19):14493–14504.
13. Sorimachi H, et al. (1995) Muscle-specific calpain, p94, responsible for limb girdle muscular dystrophy type 2A, associates with connectin through IS2, a p94-specific sequence. *J Biol Chem* 270(52):31158–31162.
14. Kinbara K, Sorimachi H, Ishiura S, Suzuki K (1997) Muscle-specific calpain, p94, interacts with the extreme C-terminal region of connectin, a unique region flanked by two immunoglobulin C2 motifs. *Arch Biochem Biophys* 342(1):99–107.
15. Kinbara K, et al. (1998) Purification of native p94, a muscle-specific calpain, and characterization of its autolysis. *Biochem J* 335(Pt 3):589–596.
16. Ono Y, et al. (2013) PLEIAD/SIMC1/C5orf25, a novel autolysis regulator for a skeletal-muscle-specific calpain, CAPN3, scaffolds a CAPN3 substrate, CTBP1. *J Mol Biol* 425(16):2955–2972.
17. Richard I, et al. (1995) Mutations in the proteolytic enzyme calpain 3 cause limb-girdle muscular dystrophy type 2A. *Cell* 81(1):27–40.
18. Richard I, et al. (2000) Loss of calpain 3 proteolytic activity leads to muscular dystrophy and to apoptosis-associated I κ B α /nuclear factor κ B pathway perturbation in mice. *J Cell Biol* 151(7):1583–1590.
19. Kramerova I, Kudryashova E, Tidball JG, Spencer MJ (2004) Null mutation of calpain 3 (p94) in mice causes abnormal sarcomere formation *in vivo* and *in vitro*. *Hum Mol Genet* 13(13):1373–1388.
20. Kramerova I, Kudryashova E, Wu B, Spencer MJ (2006) Regulation of the M-cadherin-beta-catenin complex by calpain 3 during terminal stages of myogenic differentiation. *Mol Cell Biol* 26(22):8437–8447.
21. Kramerova I, et al. (2008) Novel role of calpain-3 in the triad-associated protein complex regulating calcium release in skeletal muscle. *Hum Mol Genet* 17(21):3271–3280.
22. Kramerova I, et al. (2012) Impaired calcium calmodulin kinase signaling and muscle adaptation response in the absence of calpain 3. *Hum Mol Genet* 21(14):3193–3204.
23. Jaka O, et al. (2012) C3KO mouse expression analysis: Downregulation of the muscular dystrophy Ky protein and alterations in muscle aging. *Neurogenetics* 13(4):347–357.
24. Ojima K, et al. (2010) Dynamic distribution of muscle-specific calpain in mice has a key role in physical-stress adaptation and is impaired in muscular dystrophy. *J Clin Invest* 120(8):2672–2683.
25. Ojima K, et al. (2011) Non-proteolytic functions of calpain-3 in sarcoplasmic reticulum in skeletal muscles. *J Mol Biol* 407(3):439–449.
26. Ono Y, et al. (1998) Functional defects of a muscle-specific calpain, p94, caused by mutations associated with limb-girdle muscular dystrophy type 2A. *J Biol Chem* 273(27):17073–17078.
27. Diaz BG, Moldoveanu T, Kuiper MJ, Campbell RL, Davies PL (2004) Insertion sequence 1 of muscle-specific calpain, p94, acts as an internal propeptide. *J Biol Chem* 279(26):27656–27666.
28. Taveau M, et al. (2003) Calpain 3 is activated through autolysis within the active site and lyses sarcomeric and sarcolemmal components. *Mol Cell Biol* 23(24):9127–9135.
29. Ono Y, et al. (2006) Suppressed disassembly of autolyzing p94/CAPN3 by N2A connectin/titin in a genetic reporter system. *J Biol Chem* 281(27):18519–18531.
30. Herasse M, et al. (1999) Expression and functional characteristics of calpain 3 isoforms generated through tissue-specific transcriptional and posttranscriptional events. *Mol Cell Biol* 19(6):4047–4055.
31. Spencer MJ, et al. (2002) Stable expression of calpain 3 from a muscle transgene *in vivo*: Immature muscle in transgenic mice suggests a role for calpain 3 in muscle maturation. *Proc Natl Acad Sci USA* 99(13):8874–8879.
32. Ravulapalli R, Diaz BG, Campbell RL, Davies PL (2005) Homodimerization of calpain 3 penta-EF-hand domain. *Biochem J* 388(Pt 2):585–591.
33. Partha SK, Ravulapalli R, Allingham JS, Campbell RL, Davies PL (2014) Crystal structure of calpain-3 penta-EF-hand (PEF) domain: A homodimerized PEF family member with calcium bound at the fifth EF-hand. *FEBS J* 281(14):3138–3149.
34. Sáenz A, et al. (2011) Does the severity of the LGMD2A phenotype in compound heterozygotes depend on the combination of mutations? *Muscle Nerve* 44(5):710–714.
35. Ono Y, et al. (2010) Skeletal muscle-specific calpain is an intracellular Na⁺-dependent protease. *J Biol Chem* 285(30):22986–22998.
36. Matthews BW (2005) The structure of *E. coli* beta-galactosidase. *C R Biol* 328(6):549–556.
37. Ullmann A, Perrin D, Jacob F, Monod J (1965) [Identification, by *in vitro* complementation and purification, of a peptide fraction of *Escherichia coli* beta-galactosidase]. *J Mol Biol* 12(3):918–923. French.
38. Yang Y, Inouye M (1991) Intermolecular complementation between two defective mutant signal-transducing receptors of *Escherichia coli*. *Proc Natl Acad Sci USA* 88(24):11057–11061.
39. Swanson RV, Bourret RB, Simon MI (1993) Intermolecular complementation of the kinase activity of CheA. *Mol Microbiol* 8(3):435–441.
40. Rivero-Müller A, et al. (2010) Rescue of defective G protein-coupled receptor function *in vivo* by intermolecular cooperation. *Proc Natl Acad Sci USA* 107(5):2319–2324.
41. Hall MR, Gibson W (1997) Independently cloned halves of cytomegalovirus assemblin, An and Ac, can restore proteolytic activity to assemblin mutants by intermolecular complementation. *J Virol* 71(2):956–964.
42. Ono Y, et al. (2004) Possible regulation of the conventional calpain system by skeletal muscle-specific calpain, p94/calpain 3. *J Biol Chem* 279(4):2761–2771.
43. Davis TL, et al. (2007) The crystal structures of human calpains 1 and 9 imply diverse mechanisms of action and auto-inhibition. *J Mol Biol* 366(1):216–229.
44. Chan CK, Brignole EJ, Gibson W (2002) Cytomegalovirus assemblin (pUL80a): Cleavage at internal site not essential for virus growth; proteinase absent from virions. *J Virol* 76(17):8667–8674.
45. Loveland AN, Chan CK, Brignole EJ, Gibson W (2005) Cleavage of human cytomegalovirus protease pUL80a at internal and cryptic sites is not essential but enhances infectivity. *J Virol* 79(20):12961–12968.
46. Baum EZ, et al. (1993) Expression and analysis of the human cytomegalovirus UL80-encoded protease: identification of autoproteolytic sites. *J Virol* 67(1):497–506.
47. Dilanni CL, et al. (1993) Identification of the herpes simplex virus-1 protease cleavage sites by direct sequence analysis of autoproteolytic cleavage products. *J Biol Chem* 268(3):2048–2051.
48. Hall MR, Gibson W (1997) Assemblin homolog of herpes simplex virus type 1 retains proteolytic activity when expressed as a recombinant two-chain enzyme. *Virology* 227(1):160–167.
49. Beckmann JS, Spencer M (2008) Calpain 3, the “gatekeeper” of proper sarcomere assembly, turnover and maintenance. *Neuromuscul Disord* 18(12):913–921.
50. Takai K, Sawasaki T, Endo Y (2010) Practical cell-free protein synthesis system using purified wheat embryos. *Nat Protoc* 5(2):227–238.
51. Ono Y, et al. (2007) Comprehensive survey of p94/calpain 3 substrates by comparative proteomics—possible regulation of protein synthesis by p94. *Biotechnol J* 2(5):565–576.
52. Hayashi C, et al. (2008) Multiple molecular interactions implicate the connectin/titin N2A region as a modulating scaffold for p94/calpain 3 activity in skeletal muscle. *J Biol Chem* 283(21):14801–14814.
53. Pappas CT, Bhattacharya N, Cooper JA, Gregorio CC (2008) Nebulin interacts with CapZ and regulates thin filament architecture within the Z-disc. *Mol Biol Cell* 19(5):1837–1847.
54. Chimpanzee S, Analysis C; Chimpanzee Sequencing and Analysis Consortium (2005) Initial sequence of the chimpanzee genome and comparison with the human genome. *Nature* 437(7055):69–87.